



Riabchykov M., Furs T., Alexandrov A., Tsykhanovska I., Hulai O., Shemet V. (2023) Specified parameters in designing porous materials using magnetic nanotechnologies. *Journal of Engineering Sciences (Ukraine)*, Vol. 10(2), pp. C56–C62. DOI: 10.21272/jes.2023.10(2).c7

## Specified Parameters in Designing Porous Materials Using Magnetic Nanotechnologies

Riabchykov M.<sup>1</sup>[0000-0002-9382-7562], Furs T.<sup>1\*</sup>[0000-0002-4786-9980], Alexandrov A.<sup>2</sup>[0000-0003-3592-285X], Tsykhanovska I.<sup>2</sup>[0000-0002-9713-9257], Hulai O.<sup>1</sup>[0000-0002-1120-6165], Shemet V.<sup>1</sup>[0000-0001-8952-5097]

<sup>1</sup>Lutsk National Technical University, 75, Lvivska St., 43018 Lutsk, Ukraine;

<sup>2</sup>Ukrainian Engineering Pedagogics Academy, 16, Universitetska St., 61003 Kharkiv, Ukraine

### Article info:

Submitted: May 25, 2023  
 Received in revised form: September 18, 2023  
 Accepted for publication: September 27, 2023  
 Available online: September 29, 2023

### \*Corresponding email:

[t.furs@lntu.edu.ua](mailto:t.furs@lntu.edu.ua)

**Abstract.** The research is devoted to solving the problem of regulating the porosity parameters during the manufacturing process under magnetic field conditions. The process of synthesizing magnetic nanocomponents based on a mixture of divalent and trivalent iron oxides was given. The use of nanocomponents allowed for improving the conditions for creating porous materials. A device with adjustable magnetic induction was developed to produce porous materials in a magnetic field. The study of the porous material's structure with the nanopowder content in the magnetic field conditions showed a clear dependence of the structure on the magnetic parameters. When the content of nanocomponents increased to 0.3 %, and the magnetic field induction increased to 2.5 mT, the dispersion of pore sizes decreased by 8–10 times, the density of pores – increased by 15–20 times, and the average diameter of pores – decreased by 12–15 times. Mathematical dependencies that determine the porosity parameters for different values of the magnetic nanopowder content and the level of magnetic induction in the ring electromagnet were proposed. The obtained dependencies allowed for assigning the level of magnetic technological parameters to ensure the given porosity parameters. The developed methods of magnetic technology for creating porous materials can increase the quality and ensure the required porosity level.

**Keywords:** nanomaterials, porous structure, magnetic technologies, size dispersion.

## 1 Introduction

Porous materials are used in many industries. This fact applies to thermal insulation materials, materials for passive cooling, adsorption of hydrocarbons in petrochemicals, materials and products for energy storage, porous sensors, medical porous materials, and imitation of natural materials.

In many cases, the value of the porosity parameters, which include the average pore size, the number of pores per unit volume, and the dispersion of pore sizes, can be substantial.

In most cases, existing technologies for producing porous materials cannot provide the specified values of porosity parameters and have a relatively high level of dispersion of values.

In several studies, improving the parameters of porous and foamed materials is associated with nanotechnologies [1, 2]. A well-known approach uses nanomaterials based on a divalent and trivalent iron mixture. This approach is

currently limited to updating the characteristics of porous materials for the magnetic cleaning of liquids.

Simultaneously, using magnetic properties at the stage of creating porous materials can create conditions for controlling the process of pore formation, including creating conditions to ensure the necessary parameters.

## 2 Literature Review

Spheres of use, manufacture, and determination of parameters of porous and foamed materials are studied in several publications [3–5].

The study [6] describes the procedure for changing the thermal conductivity depending on the structure of the porous material and its fractal characteristics, particularly the structural elements' size, shape, and density.

The work [7] describes methods of chemical synthesis that create conditions for ensuring the desired pore structure, which has the best characteristics of materials for passive cooling.

The detailed pore size for the adsorption and productivity of light hydrocarbons was studied in the article [8]. The existence of an optimal pore size for these processes has been proven.

Providing the required pore sizes is very important for porous materials intended for energy storage. Ensuring the required pore sizes is substantiated [9]. Methods of synthesis of porous materials to ensure given structural parameters are discussed. The primary indicator is the capacity of porous materials.

To ensure the operation of triboelectric nanogenerators, porous materials that provide the required level of air conductivity and other electrical properties are needed [10]. These properties are related to the structure of the materials, which is desirable for the effective operation of the specified structures.

Pressure sensors with a porous structure [11] provide good characteristics under the condition of the necessary structural parameters of the materials.

The pore size is crucial for thermocatalysis processes. The paper [12] describes the production of 3D porous materials with different pore sizes, but it is unclear to what extent it is possible to control these sizes.

The pores' sizes are decisive in forming artificial body elements, particularly bones [13]. They affect both strength and biochemical properties. The size of the pores determines the effectiveness of treatment of wound infections, in particular exudate suction [14, 15].

In some cases, porous materials imitate natural structures. The properties of similar materials are related to the morphology of pores. In [16, 17], attempts were made to determine the influence of the shape, size, and orientation of pores on the mechanical and other properties of the porous material. Practical methods of providing these parameters are described very fragmentarily.

The use of magnetic porous materials with iron oxide nanoparticles to separate water and oil is described in the following several publications.

In [18], recipes for creating an effective emulsion polymer foam with magnetic properties for electronic devices were studied. The research work [19] describes foamy materials that absorb microwaves using polyurethane saturated with iron oxide nanoparticles, which are promising for use in stealth systems. Magnetomechanical porous materials are also used in active vibration reduction systems [20].

Magnetorheological materials based on a porous matrix and magnetic structural elements can be used in engineering applications, e.g., intelligent systems [21]. For the first time, the use of a magnetic field in the manufacturing process was proposed in the study [22] to regulate the parameters of foamed materials using magnetic nanopowders.

Most publications indicate the importance of creating specified pore sizes to ensure functional and mechanical properties. In particular, the pore parameters affect the porous material's ability to resist destruction [23].

The main parameters of porous materials are provided at the stage of their synthesis.

In the study [24], the effectiveness of creating porous materials for particular purposes increases due to the immobilization of enzymes. To a certain extent, the necessary structure is ensured. The study [25] describes creating porous materials using various foaming agents.

Unfortunately, the physical foaming technology using gas filling creates pores with a very wide range of sizes (from 0.9 to 30  $\mu\text{m}$ ) [26].

The synthesis of polymeric materials using porogenic solvents is described in [27]. The resulting pores appear as microspheres with a reasonably extensive size range.

Extrusion of polyethersulfone foam provides an approximate porosity of 51% and an average pore size of 5  $\mu\text{m}$  [28].

Using concentrated emulsions as a basis for creating structures with a given porosity [29], adding oil and other components to improve the structure of porous materials [30] can be the basis for practical applications.

The article [31] describes the bubble writing technology. It is claimed that it can ensure the given structure of porous materials, although this thesis was not proven.

Polymer materials occupy a special place in the system of porous materials. Polyurethane porous structures can be effectively used in regenerative medicine [32–34]. The technology of operational determination of structural parameters of polyurethane foam by measuring the speed of sound in the material is described in [35].

The possibility of regulating the size and morphology of the pores is declared with the help of emulsion polymerization using polystyrene nanoparticles [36].

Attempts to provide a given structure of porous structures using 3D printing followed by tomographic control [37, 38] should be considered exploratory.

The relevance of using magnetic nanocomponents in other industries should also be noted. They can be effective for medical purposes [37] for targeted drug delivery [38].

Prospects for using porous materials include the possibility of adjusting their parameters, particularly the size and density of pores. Modern technologies allow for adjusting these parameters to a limited extent. Technologies for creating magnetic nanomaterials can potentially influence the forces that create pores in materials, but these possibilities are not yet being used.

The study aims to determine the impact of magnetic technologies on the processes of creating porous materials, considering the use of magnetic nanomaterials based on ferric and trivalent iron oxides.

The object of research includes the process of pore formation in foamed materials containing magnetic nanocomponents under the action of a magnetic field.

### 3 Research Methodology

The synthesis process of nanopowders based on a mixture of ferric oxides takes place in a reactor using  $\text{FeSO}_4$  and  $\text{FeCl}_3$  as inputs [15]. After mixing and adding  $\text{NH}_4\text{OH}$ , a mixture of divalent and trivalent iron oxides is synthesized, forming a powder with magnetic properties (Figure 1).

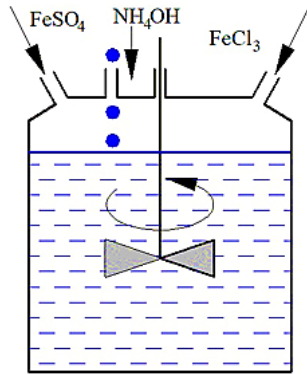


Figure 1 – The design scheme of the magnetic nanopowder synthesis

Magnetic properties compatible with the actual nano size of the powder ensure the appearance of new properties capable of determining the direction of use of such substances [39].

In most cases, producing porous materials involves their foaming, characterized by the appearance, and increase of cavities inside the material.

The experience of determining the properties of nanocomponents indicates their high adhesion combined with the ability to concentrate in the surface layer. The appearance of additional forces on the surface of the

cavities from the inside can provide the possibility of regulating the process of creation and growth of these cavities. When mixing the synthesized magnetic nanopowder with the raw material, it becomes possible to control such a process in the case of carrying out a technological process of changing inside the magnetic field.

The foaming process was carried out inside this installation by adding magnetic nanopowder to the raw material while changing the magnetic field voltage.

The magnetic field voltage  $H$ , measured in A/m, is related to the magnetic induction  $B = \mu_0 \cdot H$ , T, where  $\mu_0 = 4\pi \cdot 10^{-7}$  T/m – the magnetic constant. The force of attraction arising in this case can be defined as  $F = 0.5 \cdot A \cdot B^2 / \mu_0$ , where  $A$  – the attracted surface area.

Magnetic induction changes when the current passing through the electromagnet windings changes. At the same time, the force acting on the magnetic balls also changes. The research allows for building a diagram of the change in magnetic induction depending on the rods' separation angle.

The porous material was created by methods of foaming inside the electromagnet in addition to materials for foaming magnetic nanopowder in the ratio of 0.1, 0.2, and 0.3 % of the material mass. Simultaneously, the foaming process is carried out in a magnetic field with a voltage  $B$  of 1.0, 1.5, 2.0, and 2.5 mT.

Using magnetic nanocomponents to form porous materials in a magnetic field produced foamed polyurethane using isocyanate, polyol, and blowing agent.

The synthesis of nanopowder based on a mixture of two and trivalent iron oxides, its combination with raw materials, producing porous material under magnetic field conditions, and determining properties using microscopic studies [22] led to the results summarized in Table 1.

Table 1 – Microstructure of porous materials containing magnetic nanopowder under magnetic field conditions

| The magnetic nanocomponents content, % | $B = 1.0$ mT | $B = 1.5$ mT | $B = 2.0$ mT | $B = 2.5$ mT |
|--|--------------|--------------|--------------|--------------|
| 0.1                                    |              |              |              |              |
| 0.2                                    |              |              |              |              |
| 0.3                                    |              |              |              |              |

## 4 Results

During the experiment, magnetic nanocomponents were added to the input materials in a 0.1 to 0.3 % ratio. The foaming process took place in an annular magnetic chamber. The strength of the current in the windings of the electromagnet was changed with the help of an autotransformer and converted using the diagram “current strength – magnetic induction” into the induction of the magnetic field to ensure values in a range of 1–3 mT.

The analysis of the structure of porous materials formed under the conditions of the action of a magnetic field indicates the following:

- increasing the content of magnetic nanocomponents in the composition of raw materials for the production of porous materials increases the density of pores while reducing their average size;

- increasing the induction of the magnetic field in the presence of magnetic nanoscales significantly reduces the dispersion of the dimensional parameters of the pores. At the same time, the average pore size decreases when the density of created pores per unit volume increases.

The main parameters of the porosity during the research were determined in a unit of volume, characterized by the area within reach of the microscope objective.

Simultaneously, the average size was determined as a mathematical expectation of the pore sizes  $d_i$ , related to the average pore size in the material created without the action of a magnetic field with minimal addition of magnetic nanopowder  $d_0$ . Here and in the future, the index  $i$  refers to the number of experiments with different contents of magnetic nanocomponents and different magnetic induction. The index  $j$  – the number of separate pores.

Then, the average sizes are determined as follows:

$$d_0 = \frac{\sum_{j=1}^{N_0} d_{0j}}{N_0}; \quad d_i = \frac{\sum_{j=1}^N d_{ij}}{N}; \quad \bar{d}_i = \frac{d_i}{d_0}, \quad (1)$$

where  $d_0, d_i, d_{ij}, \bar{d}_i$  – average size measures, m;  $N_0, N$  – numbers of experiments;  $i, j$  – indexes.

The specific density of creating pores is determined by the ratio of pores in the base volume for a certain level of the content of magnetic nanocomponents and magnetic field induction to the number in the case of a minimum composition:

$$n = \frac{N_i}{N_0}, \quad (2)$$

where  $N_i$  – the number of  $i$ -the elements.

The root mean square deviation determines the variance in each individual case. For the basic version, the root mean square deviation is determined as follows:

$$\sigma_0 = \sqrt{\frac{\sum_{j=1}^{N_0} (d_0 - d_{0j})^2}{N_0}}, \quad (3)$$

where  $d_{0j}$  – the  $j$ -th diameter, m.

For an arbitrary variant, the root mean square deviation is as follows:

$$\sigma_i = \sqrt{\frac{\sum_{j=1}^{N_0} (d_i - d_{ij})^2}{N_i}}, \quad (4)$$

and the specific value of dispersion:

$$S_i = \frac{\sigma_i}{\sigma_0}. \quad (5)$$

The distribution of pores was recorded with the help of an optical microscope with a magnification of 100 times. The pore sizes were determined using a dimensional grid of a microscope.

The area that fell into the observation zone was used for analysis.

Data on the determined parameters of pore formation are given in Table 2.

Table 2 – Value of porosity parameters depending on magnetic technological parameters

| The magnetic nanocomponents content, % | Parameter     | $B = 1.0$ mT | $B = 1.5$ mT | $B = 2.0$ mT | $B = 2.5$ mT |
|--|---------------|--------------|--------------|--------------|--------------|
| 0.1                                    | $\bar{d}$ , m | 1.00         | 0.90         | 0.70         | 0.60         |
|  | $n$           | 1.00         | 1.20         | 2.10         | 2.60         |
|  | $S$ , m       | 1.00         | 0.90         | 0.60         | 0.50         |
| 0.2                                    | $\bar{d}$ , m | 0.21         | 0.18         | 0.16         | 0.14         |
|  | $n$           | 3.60         | 5.10         | 8.30         | 11.1         |
|  | $S$ , m       | 1.20         | 1.00         | 0.40         | 0.20         |
| 0.3                                    | $\bar{d}$ , m | 0.14         | 0.11         | 0.08         | 0.06         |
|  | $n$           | 6.70         | 8.90         | 15.8         | 20.1         |
|  | $S$ , m       | 1.10         | 0.80         | 0.30         | 0.10         |

The data indicate a clear dependence of the pores' size and structure on the magnetic components' content and the magnetic field's strength.

The results demonstrate a noticeable dependence on the size of the pores and the structure of their distribution depending on the nanocomponents' content and the magnetic field's strength.

The pore diameter decreases with increasing content and increasing power. At the same time, there is a clear dependence on the change in the size of the cavities, which allows for setting the necessary parameters to ensure the required dimensions.

In contrast to the known methods of creating porous materials, the proposed technology using magnetic nanocomponents can create conditions for ensuring the necessary material parameters at the process planning stage.

The obtained values make it possible to build a mathematical model of the change in the main parameters of the porous material from the technological magnetic indicators.

The general analysis of the change in the average pore diameter shows a gradual decrease with an increase in the composition of magnetic nanopowder and magnetic induction with a possible asymptotic approximation. The following function can describe such a model:

$$\bar{d} = e^{-(k_1 \cdot p + k_2 \cdot B)}, \quad (6)$$

where  $p, B$  – operating parameters;  $k_1, k_2$  – regression parameters.

Accordingly, the pore's density increases with an increase in both magnetic parameters, which the following power function can describe:

$$n = A \cdot p^{a_1} \cdot B^{a_2}, \quad (7)$$

where  $A, a_1, a_2$  – regression parameters.

The expected pore size can be found from the dependencies described by the surface in Figure 2.

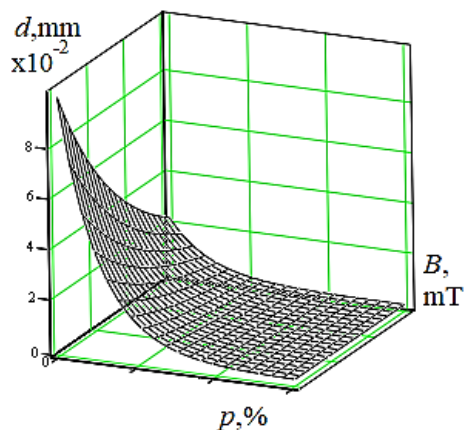


Figure 2 – The dependence of the pore size on the content of nanocomponents and magnet power

## 5 Discussion

The formation of a given structure of porous materials provides the necessary parameters of strength, porosity, water absorption, which must be specified from the conditions of use of these materials.

The values of the coefficients can be found by the method of least squares. The obtained functions allow for evaluating the magnetic technological parameters (the magnetic nanopowder content and the magnetic field induction) to achieve the specified pore sizes and their density.

The study of the strength of the obtained materials showed that this indicator depends both on the composition of the material and the method of its creation, as well as on its structure, in particular, on the average size of the pores. Similar results are obtained for thermal conductivity and hygroscopicity.

The presence of nanocomponents based on a mixture of ferric oxides significantly affects the possibility of applying magnetic technologies in creating porous materials. The process of manufacturing porous materials with magnetic nanopowder content in the conditions of an adjustable magnetic field provides variable porosity parameters.

## 6 Conclusions

Creating a variable magnetic field in ring chambers provides the necessary technological parameters.

An increase in the content of nanomagnetic components to 0.3 % with an increase in magnetic induction to 2.0–2.5 mT ensures a significant change in porosity parameters. In particular, the dispersion of pore sizes decreases by 8–10 times, the density of pores increases by 15–20 times, and the average diameter decreases by 12–15 times.

The novelty of the research is that the possibility of creating porous materials with a given structure has been proven for the first time by adding magnetic nanocomponents and foaming in a magnetic field.

The developed mathematical model allows for evaluating the parameters of the nanopowder content and magnetic field induction to ensure the specified porosity parameters.

## References

1. Javanbakht, T. (2023). Optimization of graphene oxide's characteristics with TOPSIS using an automated decision-making process. *Journal of Engineering Sciences (Ukraine)*, Vol. 10(1), pp. E1–E7. [https://doi.org/10.21272/jes.2023.10\(1\).e1](https://doi.org/10.21272/jes.2023.10(1).e1)
2. Pazini, A., Maqueira, L., Façanha, J. M. F., Pérez-Gramatges, A. (2023). Synthesis of core-shell fluorescent silica nanoparticles with opposite surface charges for transport studies of nanofluids in porous media. *Colloids and Surfaces A: Physicochemical and Engineering Aspects*, Vol. 670, 131586. <https://doi.org/10.1016/j.colsurfa.2023.131586>
3. Monie, F., Vidil, T., Grignard, B., Cramail, H., Detrembleur, C. (2021). Self-foaming polymers: Opportunities for the next generation of personal protective equipment. *Materials Science and Engineering: R: Reports*, Volume 145, 100628. <https://doi.org/10.1016/j.msere.2021.100628>
4. Suethao, S., Shah, D. U., Smitthipong, W. (2020). Recent progress in processing functionally graded polymer foams. *Materials*, Vol. 13(18), 4060. <https://doi.org/10.3390/ma13184060>



5. Pavlenko, I., Ochowiak, M., Włodarczak, S., Krupińska, A., Matuszak, M. (2023). Parameter identification of the fractional-order mathematical model for convective mass transfer in a porous medium. *Membranes*, Vol. 13(10), 819. <https://doi.org/10.3390/membranes13100819>
6. Li, W., Jiang, Y., Liu, H., Wang, C., He, X., He, F., Li, M. (2023). Mullite fibers/whiskers hierarchical porous materials: Experimental characterization and fractal model to predict thermal conductivity. *Ceramics International*, Vol. 49(9A), pp. 13657–13665. <https://doi.org/10.1016/j.ceramint.2022.12.243>
7. Yang, F., Chai, R., Zhang, J. (2023). Construction of a multi-scale microporous structure in EVA matrix toward passive cooling roofs. *Journal of Physics and Chemistry of Solids*, Vol. 178, 111358. <https://doi.org/10.1016/j.jpics.2023.111358>
8. Wang, J., Guo, Y., Luo, C., Chen, H., Pi, W., Liu, B., Yao, N., Qiu, J., Zeng, Z., Li, L. (2023). Theory-guided preparation of pore size tunable porous carbon for efficient adsorption and separation of the light hydrocarbons. *Applied Surface Science*, Vol. 623, 156941. <https://doi.org/10.1016/j.apsusc.2023.156941>
9. Yan, B., Zheng, J., Feng, L., Zhang, Q., Zhang, C., Ding, Y., Han, J., Jiang, S., He, S. (2023). Pore engineering: Structure-capacitance correlations for biomass-derived porous carbon materials. *Materials and Design*, Vol. 229, 111904. <https://doi.org/10.1016/j.matdes.2023.111904>
10. Rastegardoost, M. M., Tafreshi, O. A., Saadatnia, Z., Ghaffari-Mosanenzadeh, S., Park, C. B., Naguib, H. E. (2023). Recent advances on porous materials and structures for high-performance triboelectric nanogenerators. *Nano Energy*, Vol. 111, 108365. <https://doi.org/10.1016/j.nanoen.2023.108365>
11. Zhang, M., Xia, X., Zhang, L., Zhao, G., Liu, C., Li, N., Xu, J., Chen, Y., Jian, X. (2023). Design of healable, porous polyurethane with large ionic liquids loading amounts towards ultra-durable pressure sensor. *European Polymer Journal*, Vol. 191, 112018. <https://doi.org/10.1016/j.eurpolymj.2023.112018>
12. Wang, J., Zhang, K., Bogaerts, A., Meynen, V. (2023). 3D porous catalysts for plasma-catalytic dry reforming of methane: How does the pore size affect the plasma-catalytic performance? *Chemical Engineering Journal*, Vol. 464, 142574. <https://doi.org/10.1016/j.cej.2023.142574>
13. Morovvati, M. R., Angili, S. N., Saber-Samandari, S., Nejad, M. G., Toghraie, D., Khandan, A. (2023). Global criterion optimization method for improving the porosity of porous scaffolds containing magnetic nanoparticles: Fabrication and finite element analysis. *Materials Science and Engineering: B*, Vol. 292, 116414. <https://doi.org/10.1016/j.mseb.2023.116414>
14. Jia, X., Hua, C., Yang, F., Li, X., Zhao, P., Zhou, F., Lu, Y., Liang, H., Xing, M., Lyu, G. (2023). Hydrophobic aerogel-modified hemostatic gauze with thermal management performance. *Bioactive Materials*, Vol. 26, pp. 142–158. <https://doi.org/10.1016/j.bioactmat.2023.02.017>
15. Riabchykov, M., Tkachuk, O., Nazarchuk, L., Alexandrov, A. (2023). Conditions for the open pores formation in medical textile materials for the treatment of wounds using iron oxide nanopowders. *Materials Research Express*, Vol. 10(1), 015401. <https://doi.org/10.1088/2053-1591/acadcf>
16. Vazic, B., Newell, P. (2023). Towards the design of nature-inspired materials: Impact of complex pore morphologies via higher-order homogenization. *Mechanics of Materials*, Vol. 181, 104641. <https://doi.org/10.1016/j.mechmat.2023.104641>
17. Alazab, A. A., Saleh, T. A. (2022). Magnetic hydrophobic cellulose-modified polyurethane filter for efficient oil-water separation in a complex water environment. *Journal of Water Process Engineering*, Vol. 50, 103125. <https://doi.org/10.1016/j.jwpe.2022.103125>
18. Bury, E., Thiagarajan, S., Lazarus, N., Koh, A. (2022). Ferrofluid high internal phase emulsion polymer foams for soft, magnetic materials. *Journal of Magnetism and Magnetic Materials*, Vol. 563, 169921. <https://doi.org/10.1016/j.jmmm.2022.169921>
19. Xu, X., Tian, X., Bo, G., Su, X., Yan, J., Yan, Y. (2022). Synthesis of lightweight renewable microwave-absorbing biopolyurethane/Fe<sub>3</sub>O<sub>4</sub> composite foam: Structure analysis and absorption mechanism. *International Journal of Molecular Sciences*, Vol. 23(20), 12301. <https://doi.org/10.3390/ijms232012301>
20. Yang, J., Zhang, W., Ge, X. (2022). Preparation and magneto-mechanical properties of 3D microporous magnetorheological foam. *Journal of Intelligent Material Systems and Structures*, Vol. 34(11), pp. 1305–1313. <https://doi.org/10.1177/1045389X221131808>
21. Muhazeli, N. S., Nordin, N. A., Mazlan, S. A., Abdul Aziz, S. A., Nazmi, N. (2021). Mini review: An insight on the fabrication methods of smart magnetic polymer foam. *Journal of Magnetism and Magnetic Materials*, Vol. 534, 168038. <https://doi.org/10.1016/j.jmmm.2021.168038>
22. Riabchykov, M., Alexandrov, A., Sychov, Y., Popova, T., Nechipor, S. (2021). Magnetic nanotechnology in the production of foamed textile materials for medical purposes. *Fibres and Textiles*, Vol. 28 (3), pp. 66–71.
23. Jelitto, H., Schneider, G. A. (2020). Extended cubic fracture model for porous materials and the dependence of the fracture toughness on the pore size. *Materialia*, Vol. 12, 100761. <https://doi.org/10.1016/j.mtla.2020.100761>
24. Bharati, A., Bao Chi, K., Trunov, D., Sedlářová, I., Belluati, A., Šoóš, M. (2023). Effective lipase immobilization on crosslinked functional porous polypyrrole aggregates. *Colloids and Surfaces A: Physicochemical and Engineering Aspects*, Vol. 667, 131362. <https://doi.org/10.1016/j.colsurfa.2023.131362>
25. Bazan, P., Łach, M., Kozub, B., Figiela, B., Korniejenko, K. (2023). The production process of foamed geopolymers with the use of various foaming agents. In: *da Silva, L.F.M. (eds) Materials Design and Applications IV. Advanced Structured Materials*, Vol. 168. Springer, Cham. [https://doi.org/10.1007/978-3-031-18130-6\\_5](https://doi.org/10.1007/978-3-031-18130-6_5)
26. Park, B. K., Kim, C.-J., Kwon, D. E., Lee, Y. W. (2020). Design and fabrication of partially foamed grid structure using additive manufacturing and solid state foaming. *Processes*, Vol. 8(12), 1594. <https://doi.org/10.3390/pr8121594>

27. Maciejewska, M., Józwicki, M. (2023). Porous polymers based on 9,10-bis(methacryloyloxymethyl)anthracene – Towards synthesis and characterization. *Materials*, Vol. 16(7), 2610. <https://doi.org/10.3390/ma16072610>
28. Raje, A., Georgopoulos, P., Koll, J., Lillepär, J., Handge, U. A., Abetz, V. (2023). Open-celled foams from polyethersulfone/poly(ethylene glycol) blends using foam extrusion. *Polymers*, Vol. 15(1), 118. <https://doi.org/10.3390/polym15010118>
29. Mert, H. H., Mert, E. H. (2022). Emulsion templated hierarchical macroporous polymers. In: *Uthaman, A., Thomas, S., Li, T., Maria, H. (eds) Advanced Functional Porous Materials. Engineering Materials*, pp. 43–86. Springer, Cham. [https://doi.org/10.1007/978-3-030-85397-6\\_3](https://doi.org/10.1007/978-3-030-85397-6_3)
30. Seyrek, Y., Rudic, O., Mittermayr, F., Grengg, C., Freytag, B., Juhart, J. (2023). Impact of humidity and vegetable oil addition on mechanical properties and porosity of geopolymers. *Cement and Concrete Composites*, Vol. 140, 105083. <https://doi.org/10.1016/j.cemconcomp.2023.105083>
31. Amato, D. N., Amato, D. V., Sandoz, M., Weigand, J., Patton, D. L., Visser, C. W. (2020). Programmable porous polymers via direct bubble writing with surfactant-free inks. *ACS Applied Materials and Interfaces*, Vol. 12(37), pp. 42048–42055. <https://doi.org/10.1021/acsami.0c07945>
32. Vakil, A. U., Petryk, N. M., Du, C., Howes, B., Stinfort, D., Serinelli, S., Gitto, L., Ramezani, M., Beaman, H. T., Monroe, M. B. (2023). In vitro and in vivo degradation correlations for polyurethane foams with tunable degradation rates. *Journal of Biomedical Materials Research. Part A*, Vol. 111(5), pp. 580–595. <https://doi.org/10.1002/jbm.a.37504>
33. Holt, J. A., Torres-Sanchez, C., Conway, P. P. (2021). Monitoring the continuous manufacture of a polymeric foam via a thermokinetic-informed acoustic technique. *Proceedings of the Institution of Mechanical Engineers, Part E: Journal of Process Mechanical Engineering*, Vol. 235(6), pp. 1998–2007. <https://doi.org/10.1177/09544089211026549>
34. Abitaev, K., Qawasmi, Y., Atanasova, P., Dargel, C., Bill, J., Hellweg, T., Sottmann, T. (2021) Adjustable polystyrene nanoparticle templates for the production of mesoporous foams and ZnO inverse opals. *Colloid Polym Sci* 299, 243–258. <https://doi.org/10.1007/s00396-020-04791-5>
35. Kim, S. Y., Sesso, M. L., Franks, G. V. (2022). In-situ 4-point flexural testing and synchrotron micro X-ray computed tomography of 3D printed hierarchical-porous ultra-high temperature ceramic. *Additive Manufacturing*, Vol. 54, 102728. <https://doi.org/10.1016/j.addma.2022.102728>
36. Kanani, A. Y., Rennie, A. E. W., Bin Abd Rahim, S. Z. (2023) Additively manufactured foamed polylactic acid for lightweight structures. *Rapid Prototyping Journal*, Vol. 29(1), pp. 50–66. <https://doi.org/10.1108/RPJ-03-2022-0100>
37. Mittal, A., Roy, I., Gandhi, S. (2022). Magnetic nanoparticles: An overview for biomedical applications. *Magnetochemistry*, Vol. 8, 107. <https://doi.org/10.3390/magnetochemistry8090107>
38. Ghosal, K., Chatterjee, S., Thomas, S., Roy, P. (2023). A detailed review on synthesis, functionalization, application, challenges, and current status of magnetic nanoparticles in the field of drug delivery and gene delivery system. *AAPS PharmSciTech*, Vol. 24, 25. <https://doi.org/10.1208/s12249-022-02485-5>
39. Javanbakht, T., Laurent, S., Stanicki, D., Salzmann, I. (2021). Rheological properties of superparamagnetic iron oxide nanoparticles. *Journal of Engineering Sciences (Ukraine)*, Vol. 8(1), pp. C29–C37. [https://doi.org/10.21272/jes.2021.8\(1\).c4](https://doi.org/10.21272/jes.2021.8(1).c4)